ChemComm

COMMUNICATION

# Field effects to slow magnetic relaxation in a mononuclear Ni(II) complex†

D. Lomjanský,[a] J. Moncol',[b] C. Rajnák,[a] J. Titiš[a] and R. Boča *[a]

Cite this: *Chem. Commun.*, 2017, 53, 6930

Received 27th April 2017,
Accepted 4th June 2017

DOI: 10.1039/c7cc03275g

rsc.li/chemcomm

**A mononuclear Ni(II) complex $[Ni(NCS)_2(nqu)_2(H_2O)_2]\cdot 2nqu$ (nqu – 5-nitroquinoline) shows a field induced slow magnetic relaxation with three relaxation domains. The relaxation time for the low-frequency mode is as slow as $\tau$ = 0.3 s at $T$ = 1.9 K and $B_{DC}$ = 0.4 T.**

While data about slow magnetic relaxation in mononuclear Co(II) complexes grew rapidly in the recent period,[1] little is known about single molecule magnetism (SMM) in mononuclear Ni(II) complexes. The first SMM report on Ni(II) complexes refers to the $[Ni(pydc)(pydm)]\cdot H_2O$ complex showing a field supported slow magnetic relaxation with two relaxation channels.[2] Another report dealt with the $[Ni(mdabco)_2Cl_3]ClO_4$ complex.[3] The next neighbour, the Cu(II) complex, was disqualified for a long time by the claim that owing to the absence of an axial zero-field splitting parameter the magnetic relaxation should be fast. However, the $[Cu^{II}(pydc)(pydm)]_2\cdot H_2O$ complex shows a slow magnetic relaxation with two relaxation channels as well.[4] There are data about a slow magnetic relaxation in dinuclear $\{Cu^{II}–Eu^{III}\}$ and $\{Cu^{II}–La^{III}\}$ complexes where the slow magnetic relaxation is an inherent property of the Cu(II) centre.[5] The family of single molecule ions (SIMs) with a low spin $S$ = 1/2 is also enriched by low-spin Ni(I), Mn(IV) and V(IV) complexes.[6] The existence of a slow magnetic relaxation in low-spin systems is a task provoking revision of the generally accepted theories that SMMs can be found in systems with a high spin possessing a negative zero-field splitting parameter $D$ that causes a high-enough barrier to spin reversal $\Delta = |D|S^2$ or $\Delta = |D|(S^2 - 1/4)$ for the Kramers ions.

During the search for slow magnetic relaxation in mononuclear Ni(II) complexes we prepared the compound $[Ni(NCS)_2(nqu)_2(H_2O)_2]\cdot 2nqu$ (hereafter **1**) where nqu stands for 5-nitroquinoline. Details of synthesis, analysis and molecular spectra are provided in the ESI.†

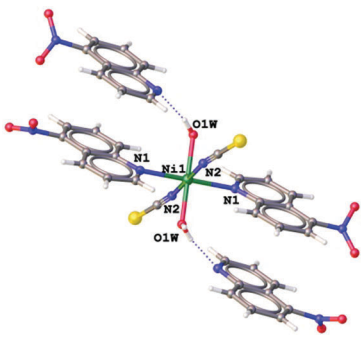


Fig. 1 Molecular structure of **1** at 100 K.

Complex **1** crystallizes in the triclinic system with the space group $P\bar{1}$. Its crystal structure consists of complex molecules $[Ni(NCS)_2(nqu)_2(H_2O)_2]$ and uncoordinated 5-nitroquinoline molecules (Fig. 1).‡ The nickel(II) central atom lies at the centre of symmetry, and is hexacoordinated by two nitrogen atoms of coordinated 5-nitroquinoline ligands [Ni1–N1 = 2.031(1) Å], two water oxygen atoms [Ni1–O1W = 2.078(1) Å], and two thiocyanato nitrogen atoms [Ni1–N2 = 2.214(1) Å]. The complex molecules and uncoordinated 5-nitroquinoline molecules are connected through O–H···N hydrogen bonds between coordinated water molecules and nitrogen atoms of uncoordinated 5-nitroquinoline molecules [$d$(O1W···N4) = 2.770(2) Å] (see Fig. S3 and Table S3, ESI†). The complex molecules are joined through O–H···S hydrogen bonds between coordinated water molecules and sulphur atoms of thiocyanato ligands of neighbouring complex molecules [$d$(O1W···S1) = 3.213(2) Å] into iron-chain like supramolecular chains (Fig. S3 and Table S3, ESI†). The coordinated and uncoordinated 5-nitroquinoline molecules are stacked (Fig. S4, ESI†). The π–π stacking interactions[7] are observed between benzene rings [C4–C9] and benzene rings [C14–C19]; between benzene rings [C4–C9] and pyridine rings [C11–C14/C19/N4]; between pyridine rings [C1–C4/C9/N1] and benzene rings [C14–C19]; and between [C1–C4/C9/N1] and pyridine rings [C11–C14/C19/N4] with centroid–centroid

[a] *Department of Chemistry, Faculty of Natural Sciences, University of SS Cyril and Methodius, 917 01 Trnava, Slovakia. E-mail: roman.boca@ucm.sk*
[b] *Institute of Inorganic Chemistry, FCHPT, Slovak University of Technology, 812 37 Bratislava, Slovakia*

† Electronic supplementary information (ESI) available: Details of synthesis, analysis, spectra, X-ray structure and calculations. CCDC 1540217. For ESI and crystallographic data in CIF or other electronic format see DOI: 10.1039/c7cc03275g

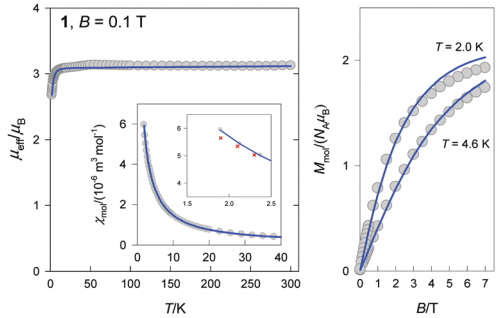


Fig. 2 DC magnetic functions for **1**. Left: Temperature dependence of the effective magnetic moment; inset: molar magnetic susceptibility, right: magnetization per formula unit. Circles: experimental data; lines: a simultaneous fit of the susceptibility and magnetization data using the standard zero-field splitting model.

distances[7] of 3.79, 3.50, 3.52 and 3.74 Å, respectively, and shift distances of 1.64, 0.90, 0.56 and 1.63 Å, respectively.

The DC magnetic data were taken with the SQUID magnetometer (MPMS-XL7, Quantum Design) between 1.9 and 300 K at an applied field of $B_{DC}$ = 0.1 T for susceptibility. Raw magnetic data were corrected for the underlying diamagnetism. The temperature dependence of the effective magnetic moment confirms a Curie-like behaviour between 300 and 20 K with almost constant $\mu_{eff}$ = 3.24 $\mu_B$; upon further cooling it drops down to a limit of $\mu_{eff}$ = 2.40 $\mu_B$ at $T$ = 1.9 K (Fig. 2). This fingerprint of the zero-field splitting (zfs) with $D < 0$ is also confirmed by the magnetization measurements since at $T$ = 2.0 K and $B$ = 7.0 T the magnetization per formula unit is only $M_{mol}/N_A$ = 1.93 $\mu_B$.

Fitting of the DC magnetic data (both susceptibility and magnetization) by the standard zfs model (see ESI†) gave $g_{iso}$ = 2.180(27), $D/hc$ = −5.86(69) cm$^{-1}$, molecular field correction $zj/hc$ = 0.020 cm$^{-1}$, and temperature-independent magnetism $\chi_{TIM}$ = 0.99 × 10$^{-9}$ m$^3$ mol$^{-1}$. Analogous predictions offer the *ab initio* calculations using the ORCA package:[8] $g_x$ = 2.220, $g_y$ = 2.224, $g_z$ = 2.277 ($g_{iso}$ = 2.240), $D/hc$ = −7.22 and $E/hc$ = 0.30 cm$^{-1}$.§

After corrections to the heterogeneous donor set, $\Delta_i = (d_i - \bar{d}_i)$, the structural distortion parameter is $D_{str} = \Delta_z - (\Delta_x + \Delta_y)/2$ = −16 pm and it matches predictions of the magnetostructural $D$-correlation.[9]

The AC susceptibility data were acquired at the amplitude of the oscillating field $B_{AC}$ = 0.38 mT.¶ The first scan refers to the field dependence of the AC susceptibility components for four representative frequencies (Fig. 3). It can be seen that at the zero field the out-of-phase susceptibility component is absent, pointing to a fast magnetic relaxation. This component is almost negligible also at $B_{DC}$ = 0.1 T. However, with increasing external field the $\chi''$ component increases but differently for different frequencies.

The frequency dependence of the AC susceptibility components for a set of DC magnetic fields between $B_{DC}$ = 0.4 and 1.4 T is displayed in Fig. 4. In all cases three relaxation domains are visible. The low-frequency channel (LF) occurs at $f < 1$ Hz which results in the fact that the relaxation time $\tau_{LF}$ is ∼0.3 s

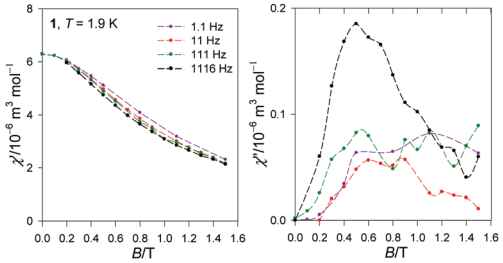


Fig. 3 Field dependence of the AC susceptibility components (SI units). Lines serve as a guide to the eye. Left: The in-phase component; right: the out-of-phase component.

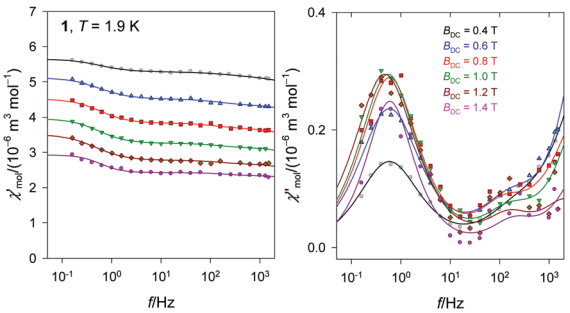


Fig. 4 Frequency dependence of the AC susceptibility components (SI units). Lines: fitted with the three-set Debye model.

($T$ = 1.9 K). At $f \sim 100$ Hz an intermediate-frequency (IF) relaxation mode is visible whereas around 1000 Hz the onset of a high-frequency (HF) channel is recognized. Two or three relaxation channels are not rare: they were identified in a number of Dy(III), Co(II) and also in Ni(II) and Cu(II) complexes.[2,4,5,10] Owing to the strong field dependence and also doping experiments the low-frequency relaxation mode has been assigned to the intermolecular interactions that create aggregates of various size;[11] upon heating these oligomers disintegrate into mononuclear entities belonging to the HF mode.

The $\chi'$ and $\chi''$ data (46 points) have been fitted by a three-set Debye model

$$\chi(\omega) = \chi_S + \sum_{k=1}^{N} \frac{\chi_k - \chi_{k-1}}{1 + (i\omega\tau_k)^{1-\alpha_k}} \quad (1)$$

($N$ = 3) containing 10 free parameters: three isothermal susceptibilities $\chi_{Tk}$, distribution parameters $\alpha_k$, and relaxation times $\tau_k$ along with the common adiabatic susceptibility $\chi_S$. While the characteristics of the LF relaxation channel are obtained reliably, the parameters for the IF and HF modes are less reliable mostly owing to the lack of HF data passing through a maximum (expected position is at $f > 10^4$ Hz); also the adiabatic susceptibility $\chi_S$ in the high-frequency limit is not fixed satisfactorily.

The difference in the height of the LF peak is significant when passing from $B_{DC}$ = 0.4 to 0.6 and 0.8 T. A further increase in the field to 1.0 and 1.2 T brings only a small effect but at $B_{DC}$ = 1.4 T a decrease in the height of the LF peak is registered.

With increasing temperature the AC susceptibility data are more scattered and thus they are hardly fitted in order to be suitable for Argand and/or Arrhenius like diagrams.

A comparison of the SIM parameters of **1** with those of two so far reported Ni(II) SIMs, the haxacoordinate complex $[Ni(pydc)(pydm)]\cdot H_2O$ (**2**) and pentacoordinate complex $[Ni(mdabco)_2Cl_3]ClO_4$ (**3**), is complicated by the fact that they depend not only on the temperature but also on the external DC field.[2,3] Usually the adiabatic susceptibility $\chi_S$ (in the high-frequency limit $f \rightarrow \infty$) decreases with temperature and also with the applied $B_{DC}$.

There are two relaxation modes in **2** with relaxation times $\tau_{LF}$ = 82 ms and $\tau_{HF}$ = 527 μs, respectively, at $T$ = 1.9 K and $B_{DC}$ = 0.2 T, and the mole fraction evaluated as $x_{LF} = (\chi_{T(LF)} - \chi_S)/(\chi_{T(HF)} - \chi_S) = 0.31$. The height of the LF peak (given by the thermal susceptibility $\chi_{T(LF)}$ on $f \rightarrow 0$) decreases progressively with temperature confirming that the mole fraction $x_{LF}$ decreases in favour of $x_{HF}$.

For **3** the AC susceptibility data were reported only for frequencies $f > 100$ Hz so that one cannot conclude about a possible LF relaxation channel below this window. However, deviations from perfect semi-circles suggest that a variety of processes contribute to the relaxation (SIM parameters are not displayed). A maximum of the out-of-phase susceptibility component at $f$ = 3000 Hz implies $\tau$(HF) = 53 μs at $T$ = 2.0 K and $B_{DC}$ = 0.2 T.

For **1** the position of the peak at the out-of-phase susceptibility component lies at $f$ = 0.6 Hz and thus $\tau$(LF) = 275(23) ms at $T$ = 1.9 K and $B_{DC}$ = 0.4 T. This is the longest relaxation time among Ni(II) SIMs reported so far. An increase in the external magnetic field to $B_{DC}$ = 1.2 T causes its prolongation to $\tau$(LF) = 336(37) ms. Notice that this system possesses only a moderate zero-field splitting parameter $D = -6$ cm$^{-1}$ unlike $D = -12$ and $-311$ cm$^{-1}$ reported previously for **2** and **3**. Thus it is less favoured for the SIM behaviour. Contrary to this disadvantage, the system possesses a very long relaxation time.

Slovak grant agencies (APVV-14-0078, APVV-16-0039 and VEGA 1/0534/16) are acknowledged for the financial support. This work was carried out with the support of the Research and Development Operational Programme for the project "University Science Park of STU Bratislava" (ITMS project no. 26240220084) co-funded by the European Regional Development Fund.

## Notes and references

‡ Crystallographic data: a single-crystal of **1** was mounted on a Stoe StadiVari diffractometer equipped with a PILATUS3R 300 K detector and a microfocus source Xenocs FOX3D Cu HD ($\lambda$ = 1.54186 Å) at 100 K. The structure of **1** was solved by SHEXTL and refined by SHELXL (ver. 2016/6). Nitro groups of 5-nitroquinoline molecules are disordered in two positions. The structure was drawn using the OLEX2 program.[12] Crystal data for **1**: $C_{38}H_{28}N_{10}NiO_{10}S_2$, triclinic $P\bar{1}$, $a$ = 8.0112(3), $b$ = 8.0734(3), $c$ = 14.9981(5) Å, $\alpha$ = 82.284(3), $\beta$ = 81.302(3), $\gamma$ = 76.188(3) deg, $V$ = 926.28(6) Å$^3$, $Z$ = 1, $D_c$ = 1.627 g cm$^{-3}$, $\mu$ = 2.473 mm$^{-1}$, $F$(000) = 466, $T$ = 100(1) K, $2\theta_{max}$ = 142.68° ($-9 \leq h \leq 7$, $-9 \leq k \leq 9$, $-18 \leq l \leq 16$). Final results (313 parameters and 3 restraints): $R_1$ = 0.0314 and w$R_2$ = 0.0883 [$I > 2\sigma(I)$], and $R_1$ = 0.0351, w$R_2$ = 0.0899 and $S$ = 1.034 for all 22 071 reflections. CCDC 1540217.†

§ The *ab initio* calculations have been performed for the whole complex in its experimental geometry using the complete active space self-consistent field (CASSCF) method improved by the second-order N-electron valence perturbation theory (NEVPT2). An active space in which eight electrons are distributed into the five nickel d-orbitals (CAS(8,5)) was employed along with the TZVP basis set for all elements. In the CASSCF procedure, the orbitals were optimized for an average of 10 triplet ($^3$F and $^3$P terms of the free Ni(II)) and 15 singlet ($^1$G, $^1$D and $^1$S terms) roots. The *D*-values were calculated through quasi-degenerate perturbation theory (QDPT) in which the spin–orbit coupling (SOC) operator (in SOMF approximation) is diagonalized on the basis of the non-relativistic SA-CASSCF/NEVPT2 eigenfunctions.

¶ Technical note: some AC susceptibility data are uncommonly scattered owing to a weak signal arising from the $S$ = 1 spin system and small amplitude of the AC field. Also fluctuations of the DC magnetic field give rise to the possible scattering. Each experimental point is an average of ten scans (each averaging four blocks) with omission of data outside the 0.7$\sigma$ interval. Data taking below $f < 1$ Hz is tedious: time to average is as long as 79 s for $f$ = 0.1 s.

1 (*a*) G. A. Craig and A. Murrie, *Chem. Soc. Rev.*, 2015, **44**, 2135; (*b*) S. Gómez-Coca, D. Aravena, R. Morales and E. Ruiz, *Coord. Chem. Rev.*, 2015, **289–290**, 379; (*c*) J. M. Frost, K. L. M. Harriman and M. Murugesu, *Chem. Sci.*, 2016, **7**, 2470 and references therein.
2 J. Miklovič, D. Valigura, R. Boča and J. Titiš, *Dalton Trans.*, 2015, **44**, 12484.
3 K. E. R. Marriott, L. Bhaskaran, C. Wilson, M. Medarde, S. T. Ochsenbein, S. Hill and M. Murrie, *Chem. Sci.*, 2015, **6**, 6823.
4 R. Boča, C. Rajnák, J. Titiš and D. Valigura, *Inorg. Chem.*, 2017, **56**, 1478.
5 M. Dolai, M. Ali, C. Rajnák, J. Titiš and R. Boča, to be published.
6 (*a*) W. Lin, T. Bodenstein, V. Mereacre, K. Fink and A. Eichhofer, *Inorg. Chem.*, 2016, **55**, 2091; (*b*) R. C. Poulten, M. J. Page, A. G. Algarra, J. L. Le Roy, I. Lopez, E. Carter, A. Llobet, S. A. Macgregor, M. F. Mahon, D. M. Murphy, M. Murugesu and M. K. Whittlesey, *J. Am. Chem. Soc.*, 2013, **135**, 13640; (*c*) M. Atzori, L. Tesi, E. Morra, M. Chiesa, L. Sorace and R. Sessoli, *J. Am. Chem. Soc.*, 2016, **138**, 2154; (*d*) M. Ding, G. E. Cutsail, D. Aravena, M. Amoza, M. Rouzières, P. Dechambenoit, Y. Losovyj, M. Pink, E. Ruiz, R. Clérac and J. M. Smith, *Chem. Sci.*, 2016, **7**, 6132.
7 C. Janiak, *J. Chem. Soc., Dalton Trans.*, 2000, 3885.
8 (*a*) F. Neese, The ORCA program system, *Wiley Interdiscip. Rev.: Comput. Mol. Sci.*, 2012, **2**, 73; (*b*) F. Neese, *ORCA – An Ab Initio, Density Functional and Semi-empirical Program Package, Version 4.0.0*, 2017; (*c*) M. Atanasov, D. Ganyushin, D. A. Pantazis, K. Sivalingam and F. Neese, *Inorg. Chem.*, 2011, **50**, 7460; (*d*) C. Angeli, S. Borini, M. Cestari and R. Cimiraglia, *J. Chem. Phys.*, 2004, **121**, 4043; (*e*) C. Angeli, R. Cimiraglia, S. Evangelisti, T. Leininger and J.-P. Malrieu, *J. Chem. Phys.*, 2001, **114**, 10252; (*f*) C. Angeli, R. Cimiraglia and J.-P. Malrieu, *J. Chem. Phys.*, 2002, **117**, 9138; (*g*) F. Neese, *J. Chem. Phys.*, 2005, **122**, 34107; (*h*) D. Ganyushin and F. Neese, *J. Chem. Phys.*, 2006, **125**, 24103; (*i*) F. Neese, *J. Chem. Phys.*, 2007, **127**, 164112.
9 J. Titiš and R. Boča, *Inorg. Chem.*, 2010, **49**, 3971.
10 (*a*) R. Boča, J. Mikovič and J. Titiš, *Inorg. Chem.*, 2014, **53**, 2367; (*b*) C. Rajnák, J. Titiš, R. Boča, O. Fuhr and M. Ruben, *Inorg. Chem.*, 2014, **53**, 8200; (*c*) A. Packová, J. Miklovič and R. Boča, *Polyhedron*, 2015, **102**, 88; (*d*) L. Smolko, J. Černák, M. Dušek, J. Miklovič, J. Titiš and R. Boča, *Dalton Trans.*, 2015, **44**, 17565; (*e*) C. Rajnák, A. Packová, J. Titiš, J. Miklovič, J. Moncol' and R. Boča, *Polyhedron*, 2016, **110**, 85; (*f*) C. Rajnák, J. Titiš, J. Miklovič, G. E. Kostakis, O. Fuhr, M. Ruben and R. Boča, *Polyhedron*, 2017, **126**, 174.
11 (*a*) W. Huang, T. Liu, D. Wu, J. Cheng, Z. W. Ouyang and C. Duan, *Dalton Trans.*, 2013, **42**, 15326; (*b*) F. Habib, I. Korobkov and M. Murugesu, *Dalton Trans.*, 2015, **44**, 6368.
12 (*a*) G. M. Sheldrick, *Acta Crystallogr., Sect. A: Found. Adv.*, 2015, **71**, 3; (*b*) G. M. Sheldrick, *Acta Crystallogr., Sect. C: Struct. Chem.*, 2015, **71**, 3; (*c*) O. Dolomanov, L. J. Bourhis, R. J. Gildea, J. A. K. Howard and H. Puschmann, *J. Appl. Crystallogr.*, 2009, **42**, 339.

 